Quasi-Steady and Unsteady Components of Aerodynamic Drag in Natural Wind Environments

Yasuyuki Onishi, Yasutaka Masumitsu*, Hiromu Shimiya

Honda R&D Co., Ltd.

Company 4630 Shimotakanezawa, Haga-machi, Hagagun, Tochigi 321-3393, Japan

*Honda Racing Corporation

1220-32 Shimokodo, Sakura-shi, Tochigi 329-1402, Japan

yasuyuki_onishi@jp.honda

yasutaka_masumitsu@jp.honda

hiromu_shimiya@jp.honda

Abstract:

This study evaluates the necessity of a turbulence generating system for assessing aerodynamic performance in natural wind environments. Various vehicle types were tested to classify the drag coefficient under turbulent flow into Quasi-steady and Unsteady components. The study revealed the limitations of current static pressure gradient correction methods and highlighted the potential for aerodynamic optimization through Quasi-steady weighting. The findings confirm that improving Quasi-steady components can reduce unsteady components, contributing to better aerodynamic performance in natural wind conditions.

Contribution: 2025 FKFS Conference on Vehicle Aerodynamics and Thermal Management
15 – 16 October 2025 | Leinfelden-Echterdingen

1 Introduction

In order to mitigate global warming, permitted CO2 emissions are being reduced in countries around the world. As a result, electric vehicles (BEVs), which do not emit CO2 while driving, are expected to become more widespread. BEVs are more energy-efficient than internal combustion engine vehicles, and most of the energy loss during driving is due to aerodynamic drag on highways. Therefore, reducing aerodynamic drag contributes to extending the range of electric vehicles [1].

Currently, the range and fuel efficiency on the label are calculated from road loads in mode drive cycles such as Worldwide-harmonized Light vehicles Test Cycle (WLTC) and The Environmental Protection Agency (EPA) drive cycles, which measure aerodynamic drag in a flow with an angle of attack of 0 degrees and very low turbulence intensity [2,3]. The road loads used for fuel efficiency dynamometer tests are measured by coasting down under ambient conditions with low wind or calculated by wind tunnel methods as in WLTC [4]. Consequently, in the aerodynamic development of vehicles, aerodynamic specifications are optimized under a flow with an angle of attack of 0 degrees and low turbulence in the wind tunnel. The road loads submitted for certification do not include the effects of natural wind because they assume no wind conditions [4]. Therefore, the difference between the drag coefficient (C_D) in the wind tunnel and the C_D with some turbulence due to natural wind may be one of the factors that cause the discrepancy between the label fuel economy and the actual fuel economy.

The characteristics of natural wind encountered by vehicles on public roads have much higher turbulence intensity and yaw angles larger than 0° compared to those in a wind tunnel [5,6,7,8,9,10]. To investigate the effect of turbulence on aerodynamic performance, several studies have been conducted to simulate turbulence using improved wind tunnel facilities, suggesting that turbulence increases aerodynamic drag in the real world [11,12]. The driving energy calculated from the aerodynamic C_D predicted from measured wind conditions was compared with the fuel consumption and the effect of natural wind on the fuel consumption was verified[13]. On the other hand, different vehicle models have different differences between the drag measured in turbulence and the weighted average drag value calculated by weighting the steady-state yaw sweep of C_D and the yaw angle probability distributions [14]. However, no studies have reported on the relationship and correlation between weighted-average drag and drag measured in turbulent flows.

The objective of this study is to determine whether a turbulence generating system (TGS) is necessary to evaluate aerodynamic performance in a natural wind environment. To the objective, several body types of vehicles were measured to classify C_D under turbulence flow conditions into Quasi-steady and Unsteady components and focused on the correlation between the Quasi-steady and Unsteady components. In the process, it was clarified the limitations of the current static pressure gradient correction method and also found it possible in proceeding with aerodynamic optimization with Quasi-steady weighting.

2 Evaluation definition

2.1 Natural Wind Parameters

Natural wind parameters are generally expressed as turbulence parameters, namely turbulence intensity (*TI*) and vortex scale length (*TL*). *TI* is expressed as the standard deviation of each velocity component relative to the mean velocity. Meanwhile, vortex scale length is expressed as the product of the inverse of the representative vortex frequency and the mean velocity as shown in Figure 1. These values change due to the influence of natural convection, the road environment, and surrounding vehicles, and various values are measured depending on the location. The wind has three components, u,v,w thus there are three *TI*, *TIu*, *TIv*, *TIw*. However, from the Aerodynamic Drag points of view, *TIv* is the domain parameter [11] and hereafter, The discussion focus on *TIv*.

①*TI* [%] $= \dfrac{\text{Standard deviation}}{\text{Mean Velocity}}$

②*TL*[m] = Representative Vortex length [m]
= 1/Representative Vortex frequency[s]
× Mean Velocity[m/s]

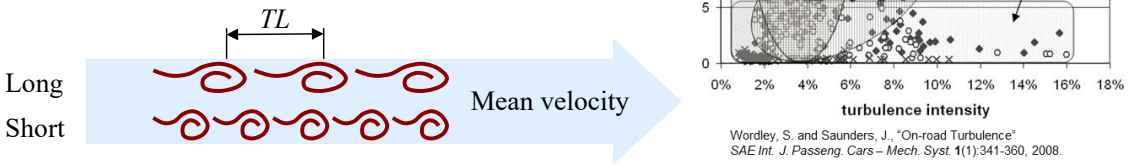

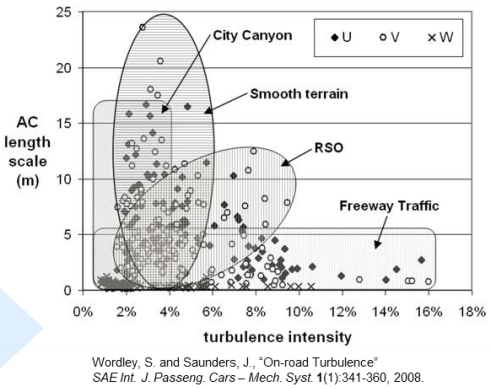

Figure 1 : Natural wind parameters [5]

In places with many structures and surrounding vehicles, turbulence intensity tends to be high and vortex scale length tends to be short. For example, on the highway road in the city. Conversely, in flat or open areas with few surrounding vehicles, turbulence intensity tends to be low and vortex scale length tends to be long. Past research has reported that turbulence intensity on roads is on the order of a few percent, and vortex scale length is often less than 10m. For example, on the smooth terrain [5].

2.2 Definition of Turbulence CD

It is assumed that the turbulent C_D can be divided into a Quasi-steady component and an Unsteady component. As shown in Figure 2, the C_D obtained from a turbulence flow with turbulence intensity and vortex scale length is defined as the turbulent C_D. The Quasi-steady component is the difference between C_D measured under low turbulence with Yaw 0degree and C_D calculated by weighting the steady state Yaw sweep of the C_D by the Yaw probability distributions of the turbulence flow, weighted C_D. It is calculated by multiplying the frequency of each angle by the C_D of that angle over all angles. The Unsteady component is the difference between the weighted C_D and the turbulent C_D. In other words, the delta C_D component that cannot be explained by the Quasi-steady component is defined as the Unsteady component. Hereafter, delta C_D is expressed as dC_D.

It is considered that the Quasi-steady component mainly depends on the turbulence intensity, while the Unsteady component depends on the vortex scale length.

Turbulence intensity is defined as the ratio of the standard deviation to the mean velocity. If the turbulence is isotropic, each velocity component is likely to have a normal distribution, and the standard deviation is equivalent to the Yaw probability distribution.

The weighted C_D that is the basis of the Quasi-steady component is calculated from the Quasi-steady state Yaw sweep of C_D and the Yaw probability distribution. The Quasi-steady component is determined by the turbulence intensity, which is the standard deviation.

Therefore, it can be said that the Unsteady component is caused by the vortex scale length, which is a parameter other than the turbulence intensity. Hereafter, C_D 0.001 is expressed as 1ct.

In order to evaluate the Unsteady components that cannot be explained by the Quasi-steady components, it is necessary to measure the turbulent C_D under turbulent conditions in a wind tunnel that can generate turbulence, and compare it with the weighted C_D under the turbulent conditions, that is, the Yaw probability distribution under the turbulent conditions and the C_D Yaw sweep integration under steady input. To do this, evaluation in a wind tunnel with a turbulence generator system is required, for example, FKFS side wind generator (FKFS ***swing***) [15].

.

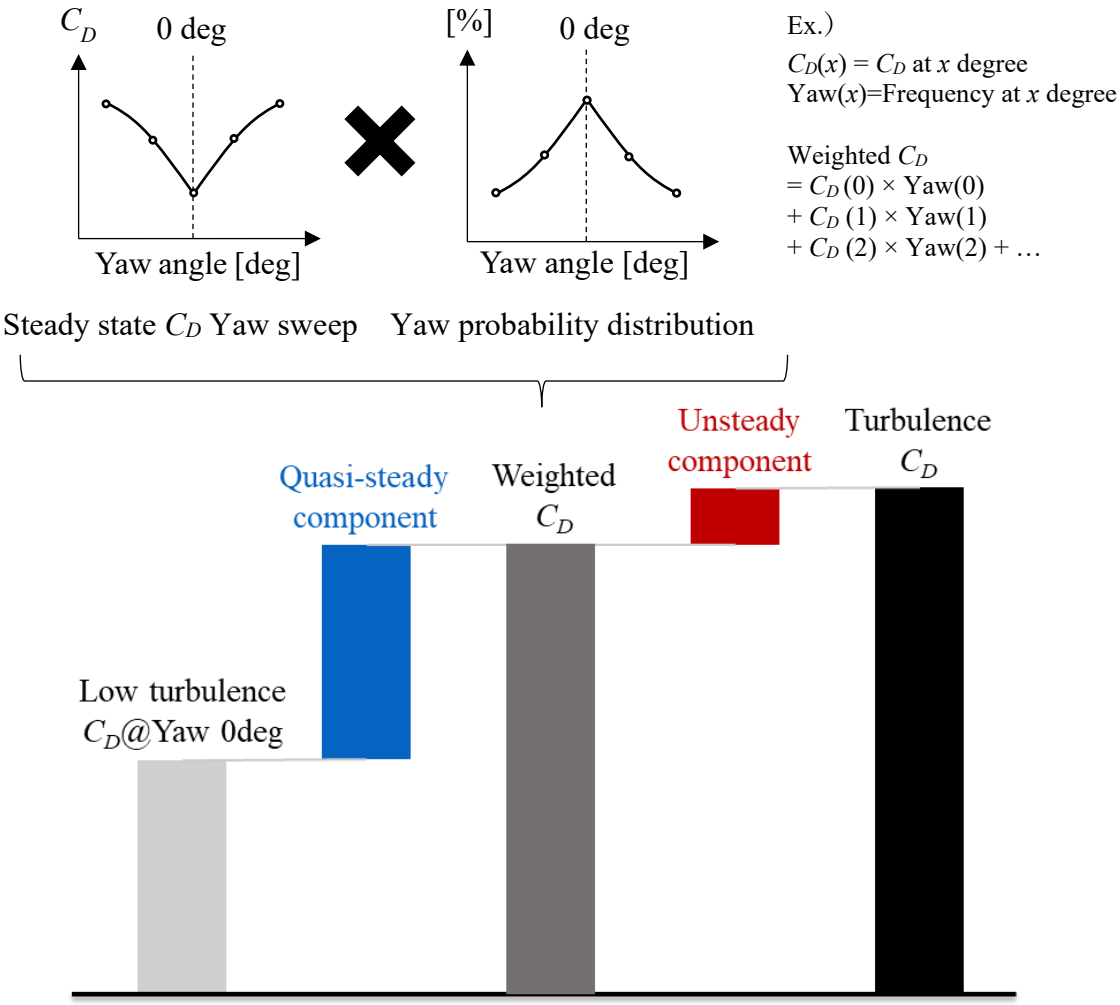

Figure 2 : Definition of Turbulence and Weighted C_D components

2.3 Static pressure gradient change and correction when using Turbulence Generation System

Generally, when the static pressure is different between the front and the end of the test vehicle, it is applied the correction for measured C_D in a wind tunnel to evaluate it without the effect from the horizontal buoyancy.

Figure 3 shows the static pressure gradient under several swing mode in FKFS scale wind tunnel. As Figure 3 shown, When the swing operates, the static pressure gradient in the X direction is changed by the movement of the turbulence generator, because the kinetic energy of the fluid added by the flap is converted into pressure for the mainstream velocity to be a constant value in the collector. Therefore, the change in the static pressure gradient becomes greater as the kinetic energy input into the mainstream becomes greater, for example, the higher the frequency with the flap operating of the same angle, the static pressure increases more near the corrector.

In this study, FKFS side wind generator (FKFS ***swing***) [14] consisting of flaps with a constant section shape in the Z direction is used. Even so, since the static pressure gradient differs depending on the turbulence mode as shown in Figure 3, it is necessary to measure the static pressure gradient and correct the impact on C_D for each turbulence condition.

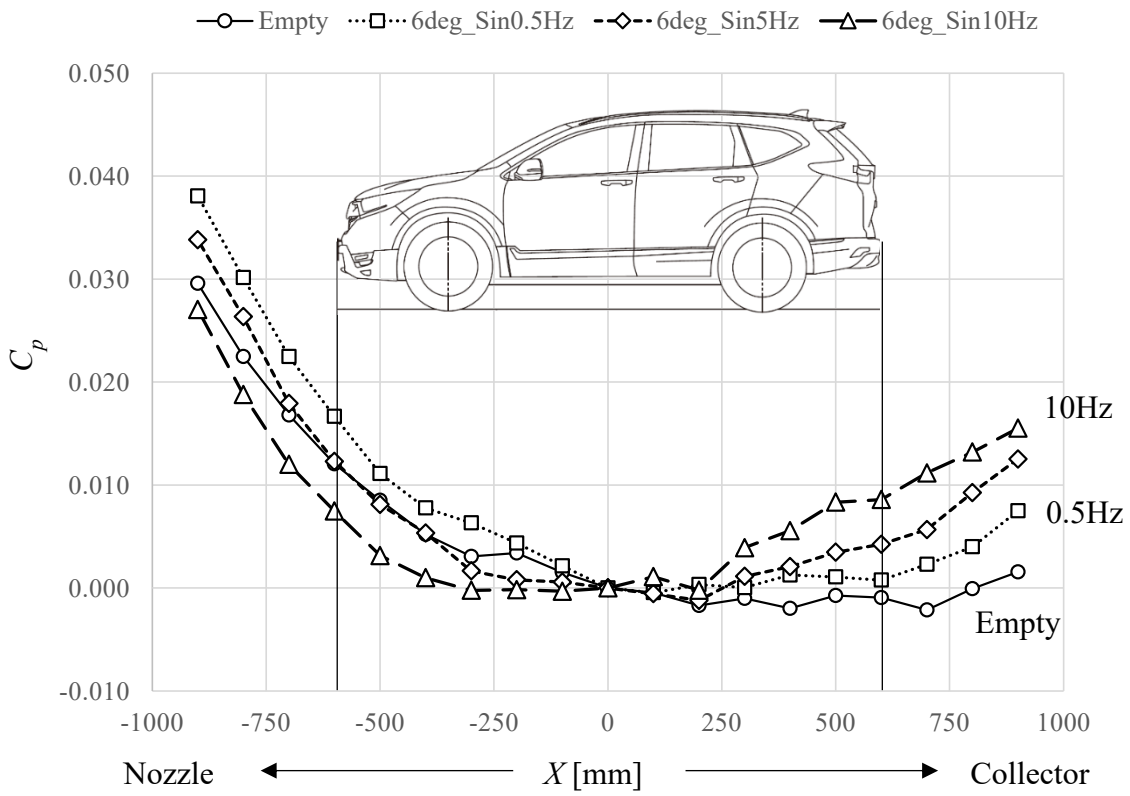

Figure 3 : Static pressure gradient at each ***swing*** mode

3 Methodology

3.1 Test vehicles

Three different body type vehicles, sedan, hatchback, and SUV were chosen to represent the flow structure from aerodynamic points of view. Sedan and hatchback have three aero options by combination of aerodynamic components to change the yaw characteristics. Figure 4 shows the C_D yaw sweep on these test vehicles with options. The absolute C_D and yaw trend are different from each other.

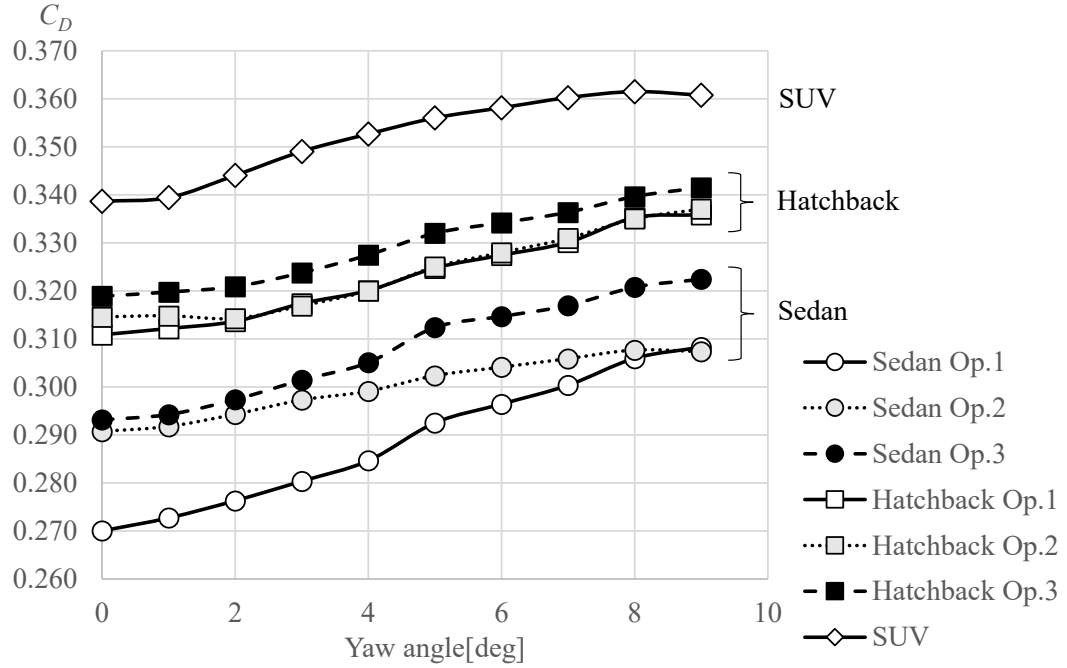

Figure 4 : C_D yaw sweep on these test vehicles with options

3.2 FKFS *swing* mode

In order to simulate as it is and simplify the natural wind condition measured on Japanese highway [11], 16 different modes were used to evaluate the relationship between Quasi-steady component and Unsteady component.

Two random modes are used to simulate the natural wind as it is in Japanese highway, which modes have *TIv* 2.6%, *TLv* 3m and *TIv* 2.2%, *TLv* 2m respectively. And Sin signal with flap angle 3 and 6 degrees from 0.4Hz to 1Hz. The flap angles were determined based on measurements, from 1σ at 3 degrees to 3σ at 6 degrees. The frequency range was also adjusted to the vortex scale length on the road. 0.4-1Hz corresponds to a vortex scale length of 5-13m, covering the range in which it mainly occurs in measured data.

4 Result

4.1 The relationship between Quasi-steady component and Unsteady component with static pressure gradient correction.

Figure 5 shows the relationship between Quasi-steady component and Unsteady component. These results were corrected for the effect of horizontal buoyancy caused by static pressure gradient. Although Two-measurement correction method was reported, here the simple correction method, which is calculated from the static pressure difference between the front and rear of the test vehicle as shown in Figure 4, is used. The correlation between the Quasi-steady and Unsteady components seems to be low and there seems to be little physical relationship between them. That means it is impossible to predict the Unsteady component impact from the Quasi-steady component.

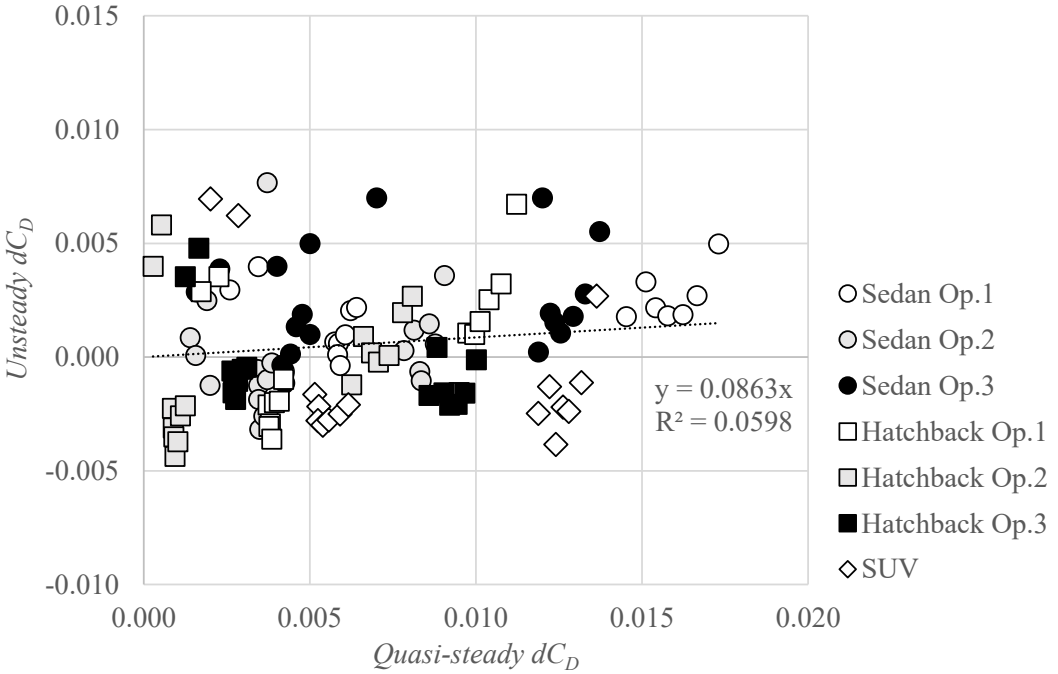

Figure 5 : The relationship between Quasi-steady component and Unsteady component measured at FKFS FSWT

4.2 Test results at Honda scale wind tunnel with Turbulence Generation System

4.2.1. Turbulence Generation System at Honda scale wind tunnel

In order to investigate the cause of Unsteady component, Honda installed Turbulence Generation System similar to FKFS ***swing*** to Honda scale wind tunnel as shown in Figure 6. Honda scale wind tunnel is designed to use 25% scale model with 5 belt rolling road system. The nozzle size is 2.3m width and 1.3 m height, and the test section length is 4.8m. The corrector size is 3.5m width and 1.9m height.

The turbulence generation system is installed at the exit of the nozzle and totally 12 flaps are installed inside the nozzle. The flap section keeps the constant section shape through the Z directions. Each flap is controlled by the motor mounted at the top of the nozzle individually. Therefore, as system, not only sin wave, but also random wave can be generated. Also, each flap can be operated individually. The flap is made of Carbon Fiber and designed the eigenfrequency over 20Hz. The weight is controlled within 2.5kg at each flap.

Maximum target averaged wind speed is limited up to 160kph. This is because the flow speed changes within 20km/h around the average wind speed, and depending on the time, the maximum wind speed approaches 190kph, which is the limit of the fan motor power. This system can generate not only v-component fluctuations, but also u-component fluctuations by changing the nozzle exit area using the two outer flaps at each. Maximum excitation frequency by this system is designed up to 10Hz and maximum flap angle is designed up to 12degrees.

The enough test section length and corrector size can achieve the flat static pressure gradient within *Cp* 0.002 from -800mm to +800mm in the X direction on the centreline at 250mm height from the ground at the balance centre as shown in Figure 7. The static pressure gradient in the Honda scale wind tunnel has been scaled up to full scale and aligned with the model.

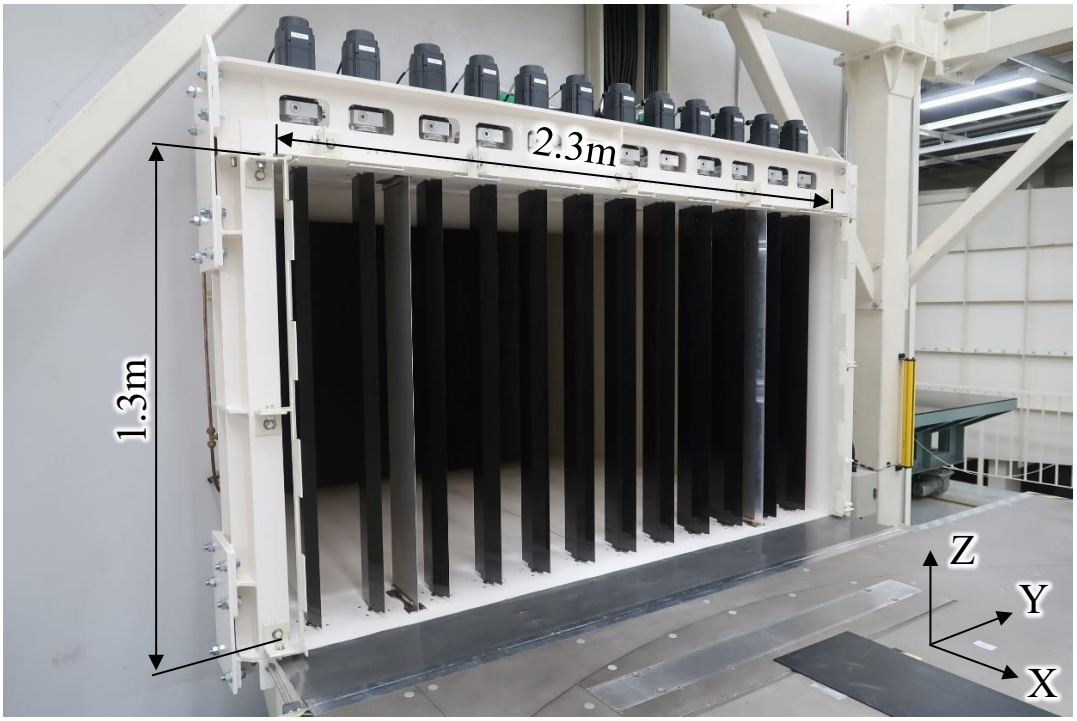

Figure 6 : Turbulence Generation System at Honda Scale Wind Tunnel

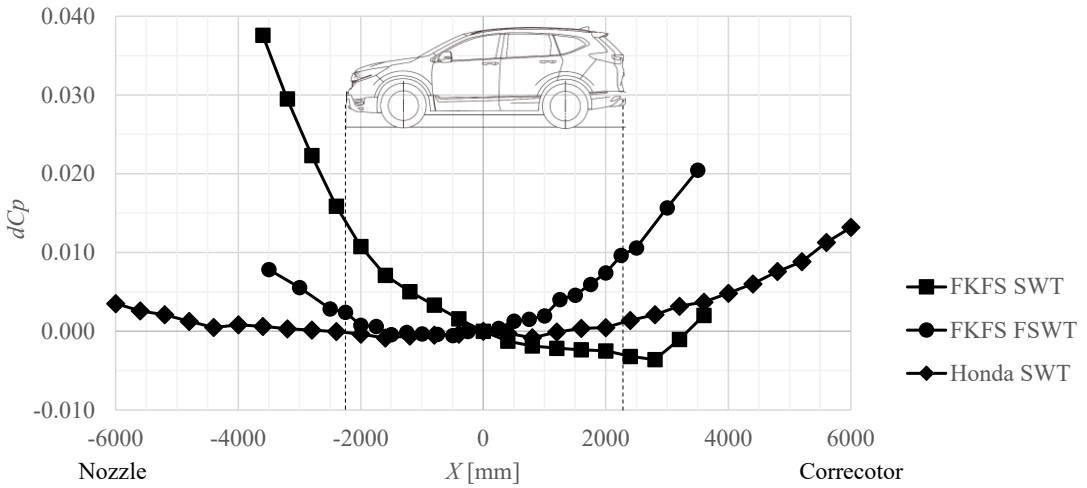

Figure 7 : Static pressure gradient comparison

4.2.2. Effect of static pressure gradient under TGS mode at each wind tunnel

Figure 8 shows the static pressure gradient results for the Honda scale wind tunnel, the FKFS scale wind tunnel, and the full-scale wind tunnel with ***swing***/TGS OFF and in a certain TGS mode (*TIv*6%, *TLv*10m). It shows that the static pressure gradient in FKFS WT decreases on the nozzle side and increases on the collector side when TGS is ON. On the other hand, in the Honda scale wind tunnel, the change in the static pressure gradient due to TGS operating is small.

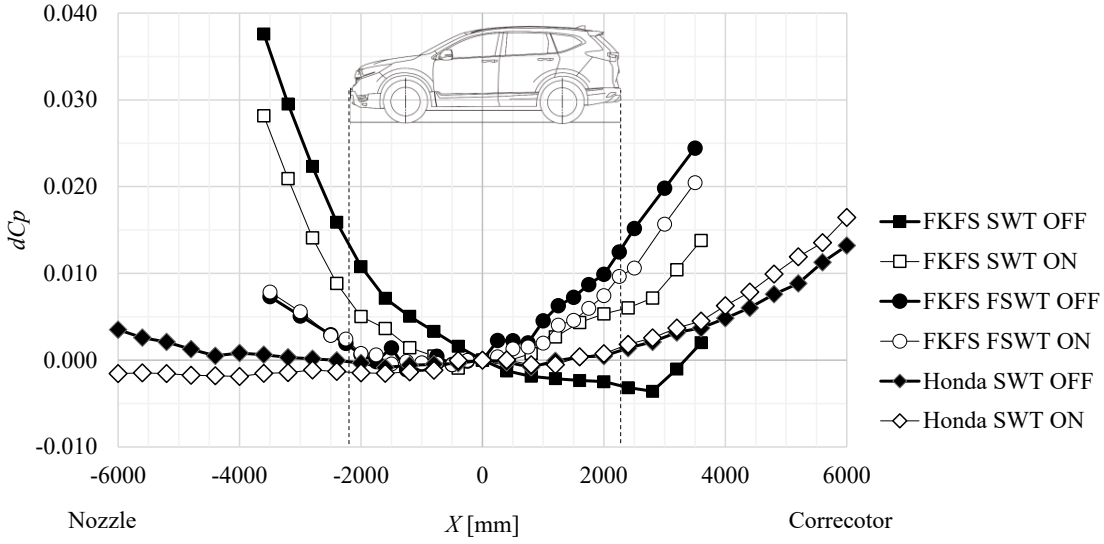

Figure 8 : Static pressure gradient under ***swing***/TGS operating mode

Figure 9 shows the value of the static pressure gradient correction with various *TIv* differences at each wind tunnel. *TLv* is about 1-2m. The horizontal axis shows *TIv*, and the vertical axis shows the static pressure gradient correction value. The static pressure gradient correction here is the static pressure difference at the front and rear positions of the vehicle.

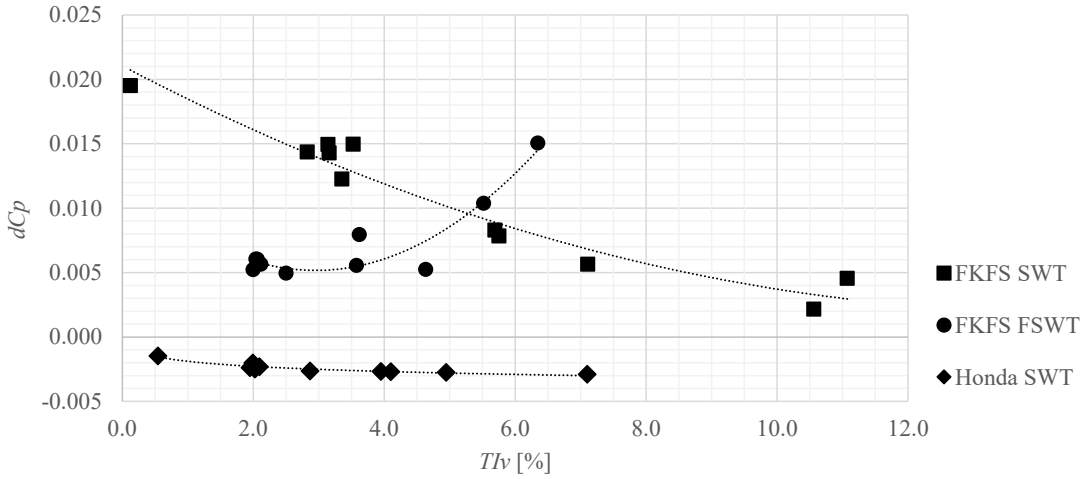

Figure 9 : The static pressure gradient correction on test vehicle Sedan through TIv differences

It can be seen that the static pressure gradient correction changes significantly depending on *TIv* in both the FKFS scale wind tunnel and the full scale wind tunnel. In addition, the tendency for the increase in *TIv* is opposite for scale wind tunnel and full scale wind tunnel. On the other hand, the static pressure gradient correction value of the Honda scale wind tunnel is almost constant regardless of the change in *TIv*, and the correction value is small at 1-3ct, which shows that the effect of the static pressure gradient due to TGS operation is small regardless of *TIv*. Although it is not possible to provide a physical basis for this difference, a hypothesis can be stated based on circumstantial evidence of the dimensions.

Table 1 shows a comparison of dimensions between the FKFS Full scale wind tunnel and scale wind tunnel, and the Honda scale wind tunnel. The scale wind tunnel dimensions are converted to full-scale dimension. It can be seen that the nozzle size, test section length, and collector size of the Honda scale wind tunnel are more than 50% larger than those of the FKFS. As mentioned earlier, the kinetic energy added by the TGS leads to an increase in pressure in the collector, so if the collector size is large and the distance to the model is long, there is less pressure propagation, and so it can be inferred from the comparison of dimensions that operating the TGS in the Honda scale wind tunnel has less impact on the static pressure gradient.

Table 1 : Comparison of dimensions between the FKFS Full scale wind tunnel and scale wind tunnel, and the Honda scale wind tunnel

Dimensions	FKFS		Honda
	SWT	FSWT	SWT
Nozzle width(m)	6.3	5.8	9.2
Nozzle Height(m)	4.2	3.9	5.2
Nozzle Area(m^2)	26.5	22.4	47.8
Nozzle to tunr table center(m)	4.7	4.6	8.8
Turn table center to Collector(m)	5.6	5.4	9.2
Test section(m)	10.3	10.0	19.2
Collector Area(m^2)	31.2	26.9	106.4

4.3 Relationship between Quasi-steady and Unsteady component

It is compared that the results measured in Honda scale wind tunnel and that in FKFS scale wind tunnel with and without static pressure gradient correction. The turbulence intensity conditions by TGS were set to be similar range for Honda scale wind tunnel and FKFS scale wind tunnel. And the turbulence scale length was about 2m for both. The wind speeds are 180kph for FKFS and 160kph for Honda. These data were measured by exactly the same Sendan model.

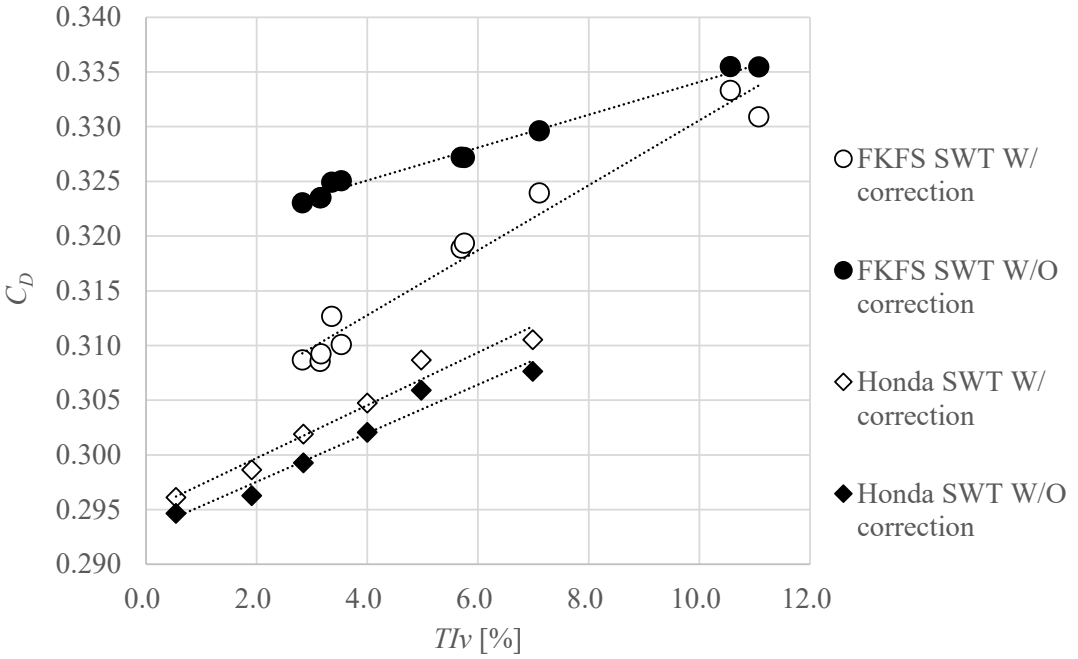

Figure 10 : The relationship between *TIv* and C_D with and without static pressure gradient correction

Figure 10 shows the relationship between *TIv* and C_D with and without static pressure gradient correction. Regardless of whether or not static pressure gradient correction is applied, C_D tends to increase as *TIv* increases. Also, the static pressure gradient correction is small due to the *TIv* difference in the Honda scale wind tunnel, so the slope is almost the same with and without correction. On the other hand, The FKFS scale wind tunnel results show that the increase in C_D versus *TIv* and the slope are different depending on whether or not correction is applied. Figure 11 shows the relationship between *TIv* and the Quasi-steady component with and without static pressure gradient correction. Honda scale wind tunnel results shows that the changes in the Quasi-steady component on TIv with and without correction are almost the same that they overlap. The FKFS scale wind tunnel results show the offset, but the changes in the influence of the Quasi-steady component on *TIv* follow the same trend. The Quasi-steady component is determined by the Yaw frequency (*TIv*), so the trend shall be the same. The offset is determined by the static pressure gradient correction value.

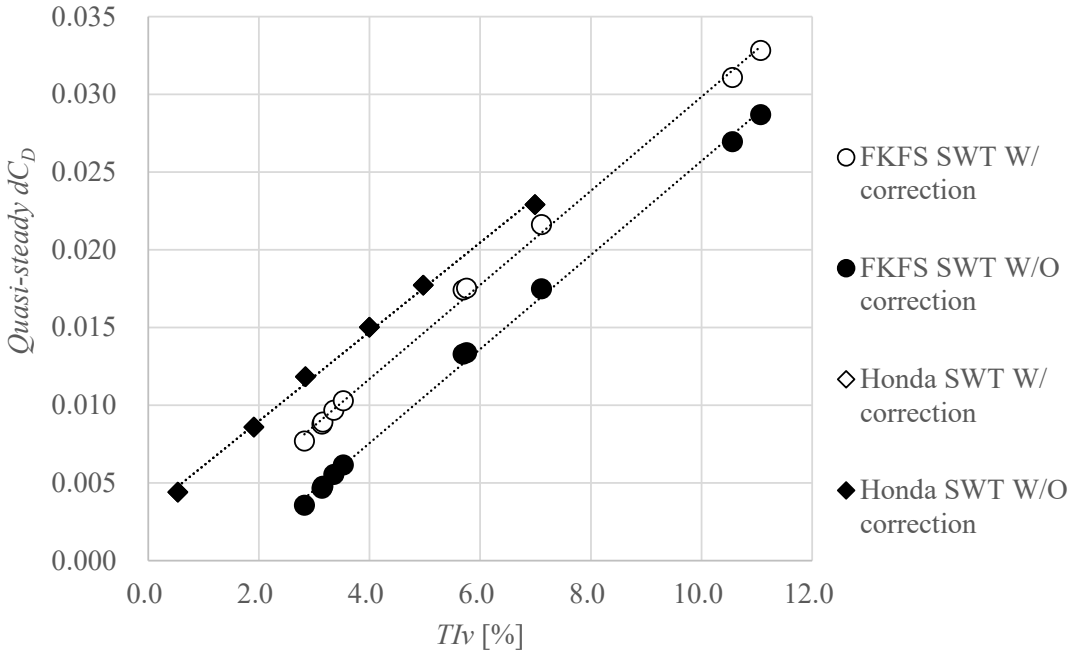

Figure 11 : The relationship between *TIv* and the Quasi-steady component with and without static pressure gradient correction

Figure 12 shows the relationship between *TIv* and Unsteady component with and without static pressure gradient correction. Honda scale wind tunnel results shows that the changes in the Unsteady component on *TIv* with and without correction are almost the same that they overlap. Because the correction value remains almost the same in the Honda wind tunnel. And also, the influence of the Unsteady component increasing in the negative direction as *TIv* increases. FKFS scale wind tunnel results show that the tendency of the Unsteady component is clearly different with and without the static pressure gradient correction value. With static pressure gradient correction, it becomes almost constant, but without static pressure gradient correction, the negative effect of the Unsteady component becomes larger as the *TIv* increases like with Honda.

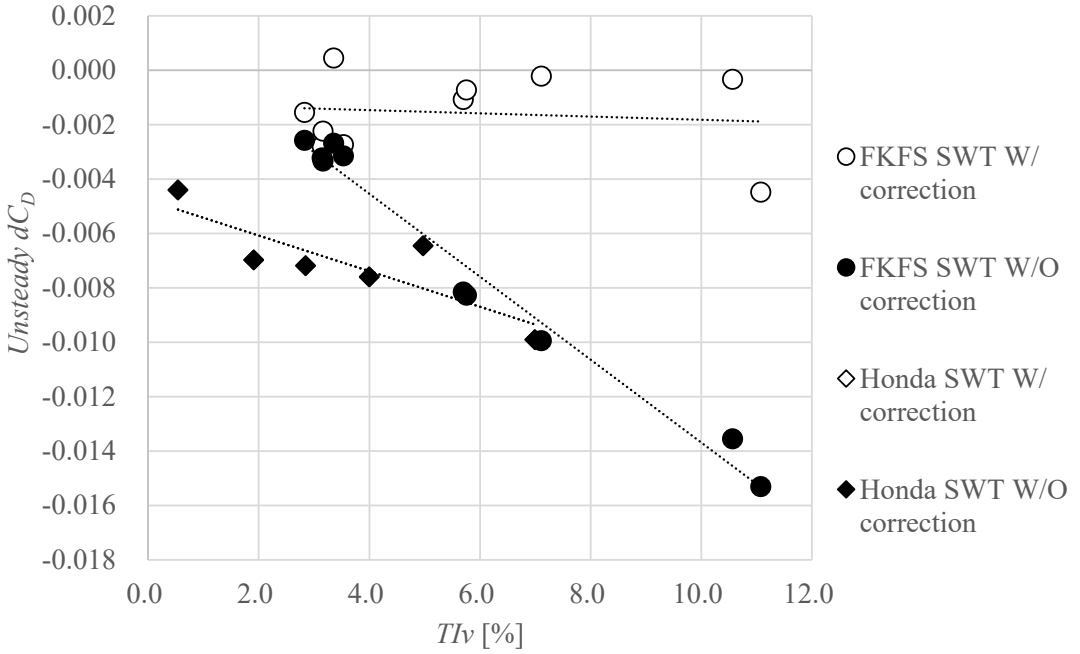

Figure 12 : The relationship between *TIv* and Unsteady component with and without static pressure gradient correction

Finally, Figure 13 shows the relationship between the Quasi-steady component and the Unsteady component. Regardless of whether a static pressure gradient correction is applied or not, Honda scale wind tunnel results show that as the Quasi-steady component decreases, the Unsteady component approaches zero. On the other hand, for the FKFS results, the results without static pressure gradient correction show that as the Quasi-steady component decreases, the Unsteady component approaches zero like the Honda scale wind tunnel results. From this, although it cannot be explained from a physical phenomenon, it is possible that the static pressure gradient correction in FKFS is not working as theoretically expected. The static pressure gradient was measured using a pitot probe while the TGS was in operation, with a measurement time of 60 seconds for each measurement point, but it is possible that the actual static pressure gradient was not captured correctly.

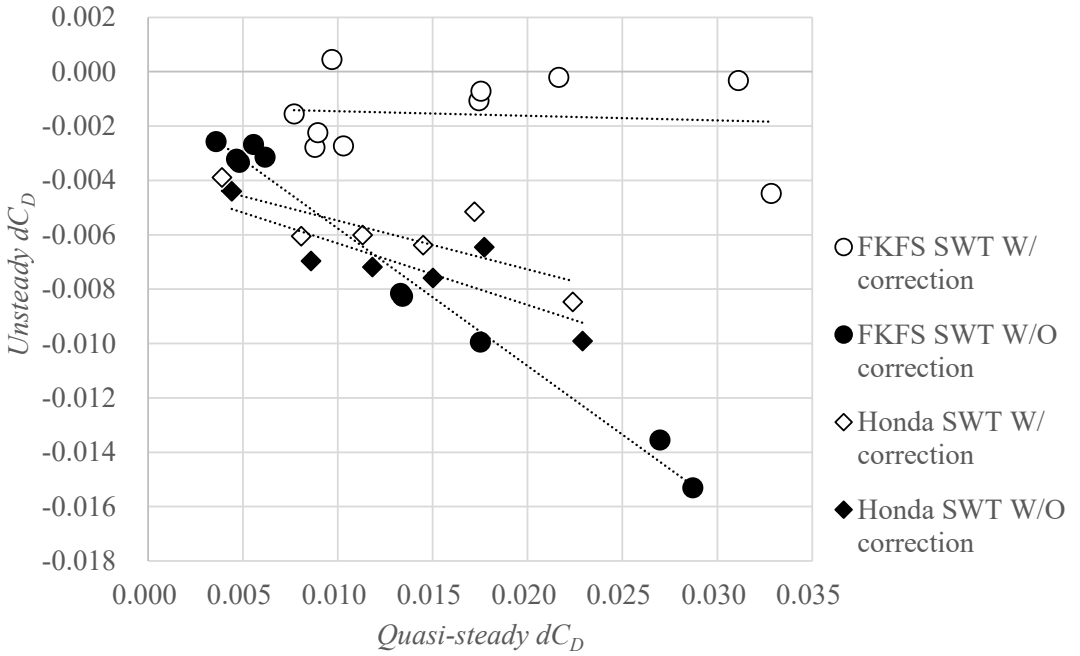

Figure 13 : The relationship between the Quasi-steady component and the Unsteady component

Assuming that static pressure gradient correction is not working properly with TGS ON, Figure 14 shows again the relationship between the Quasi-steady and Unsteady components for different vehicle types and models in the FKFS full scale wind tunnel without static pressure gradient correction. Without applying the static pressure gradient correction, it seems to be a linear relationship between the effects of the Quasi-steady and steady components. And also, it can be seen that as the Quasi-steady component becomes smaller, the Unsteady component also becomes smaller. In terms of general understanding of the phenomenon, it is natural to think that the less yaw sensitivity there is and the less likely separation will occur due to yaw changes, in other words, the smaller the influence of the Quasi-steady component, the less likely Unsteady separation phenomena will occur.

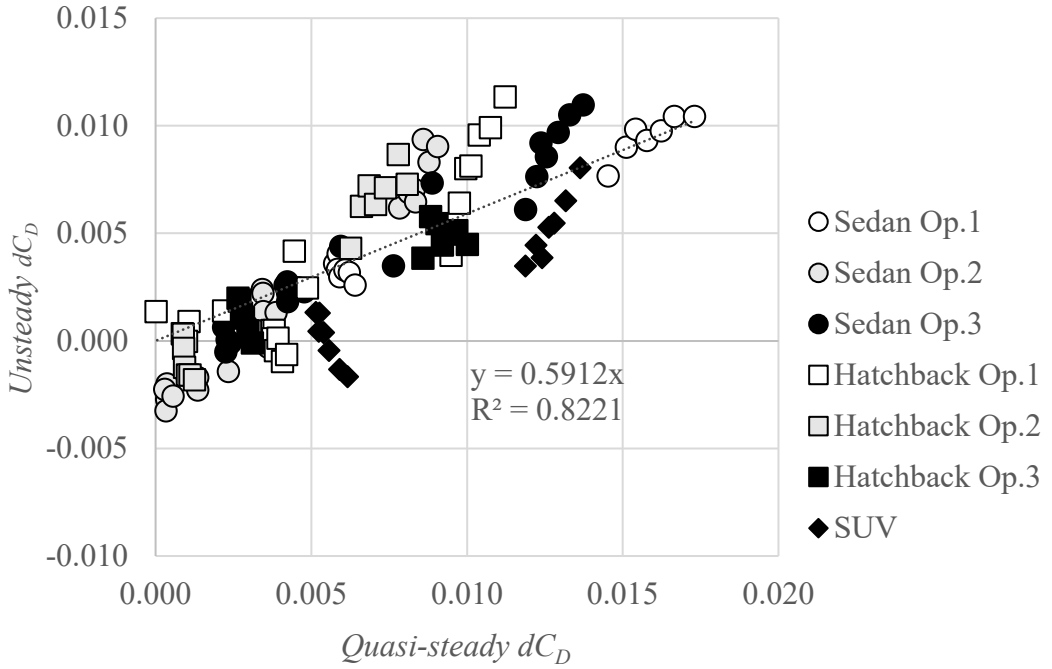

Figure 14 : The relationship between the Quasi-steady and Unsteady components in the FKFS full scale wind tunnel without static pressure gradient correction

In order to investigate where the Quasi-steady and Unsteady components appear in the flow around the vehicle, it was measured that the total pressure distribution in the WAKE behind the vehicle in the Honda model wind tunnel and identified the areas where the effects of each were apparent. The methodology how to isolate the Quasi-steady and Unsteady component from total pressure distribution is the same way of thinking as weighed C_D and Turbulence C_D. The measurements were conducted under the turbulence and steady flow at each yaw angle rotated by Turn table of the balance. Then Quasi-steady component of total pressure distribution is calculated from total pressure distribution in the WAKE behind the vehicle at each yaw angle and the yaw probability of the turbulence mode. Then, the Unsteady component is calculated by subtracting the Quasi-steady component from the pressure distribution under turbulent flow. The position of the total pressure measurement probe was calculated and adjusted to match the change in position of the model due to rotation on the turntable so that the position of the probe would be the same relative to the model.

Figure 15 shows the relationship between Quasi-steady component(dC_D) and Unsteady component(dC_D) of three test models measured at Honda scale wind tunnel under *TIv* 5% and *TLv* 1.5m. Two test models are different sedan with several aero options and One Hatchback model with several aero options. Similar to the results shown in Figure 14, there is a correlation between a reduction in the Quasi-steady component and a reduction of the Unsteady component. Op.1 and Op.2 were picked up to measure the total pressure in WAKE behind the vehicle in order to clarify the difference of both from the same vehicle model. Both Options are the same hatchback model, but with the different aerodynamic parts. Figure 16 shows C_D Yaw sweep on both options and the increase in C_D with increasing yaw angle in Op.2 is suppressed compared to Op.1. Therefore, in these test configurations Op.1 delta turbulence C_D is +6ct, Op.2 delta turbulence C_D is -1ct at each and there is clear difference between of both under turbulence.

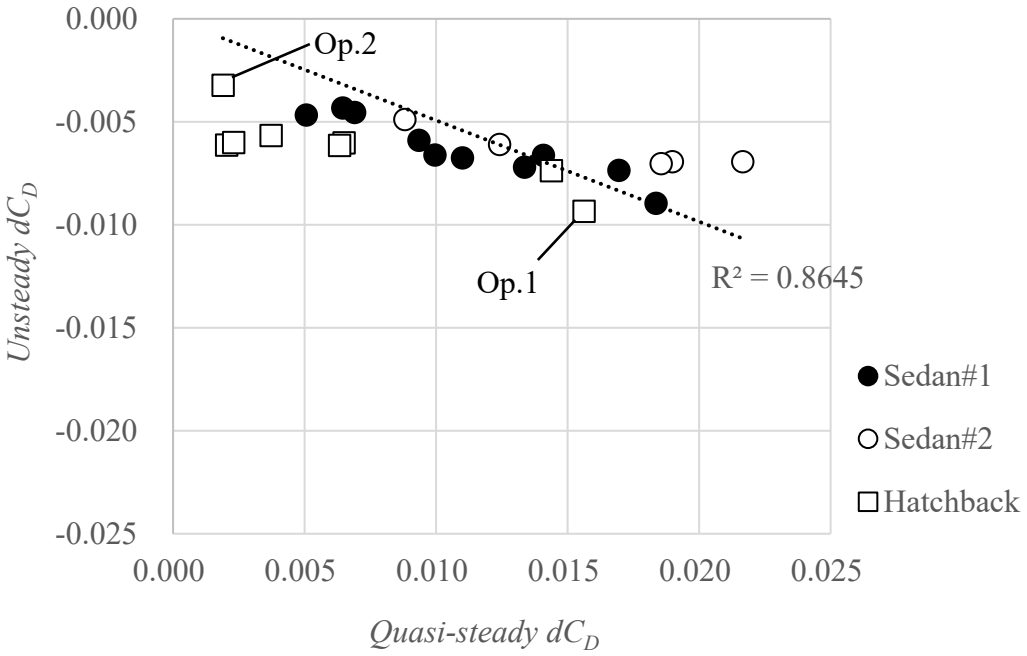

Figure 15 : The relationship between Quasi-steady component and Unsteady component of three test models measured at Honda scale wind tunnel.

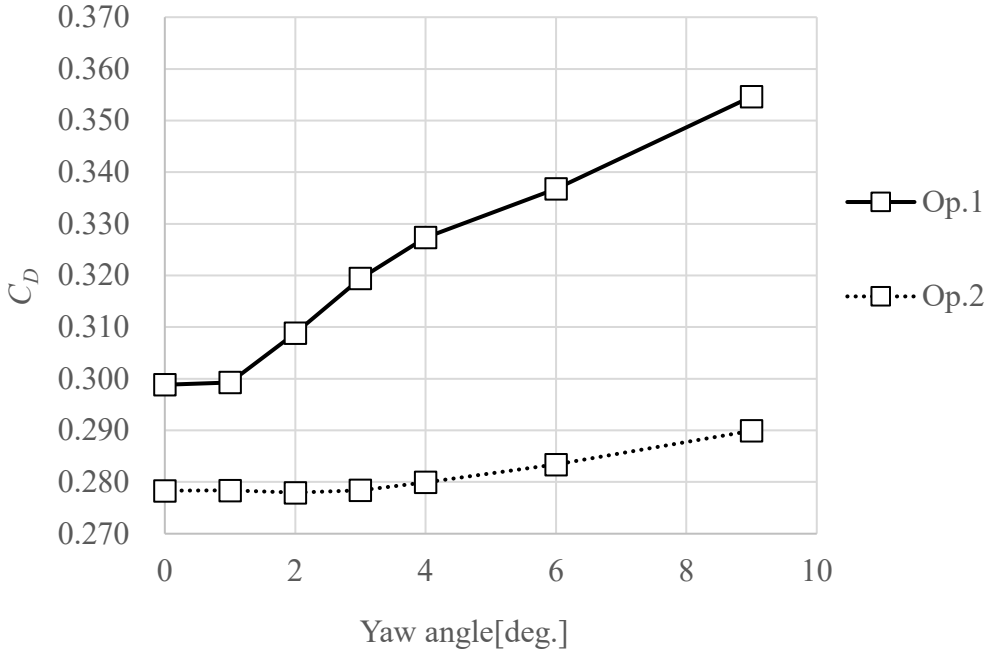

Figure 16 : C_D Yaw sweep on both options

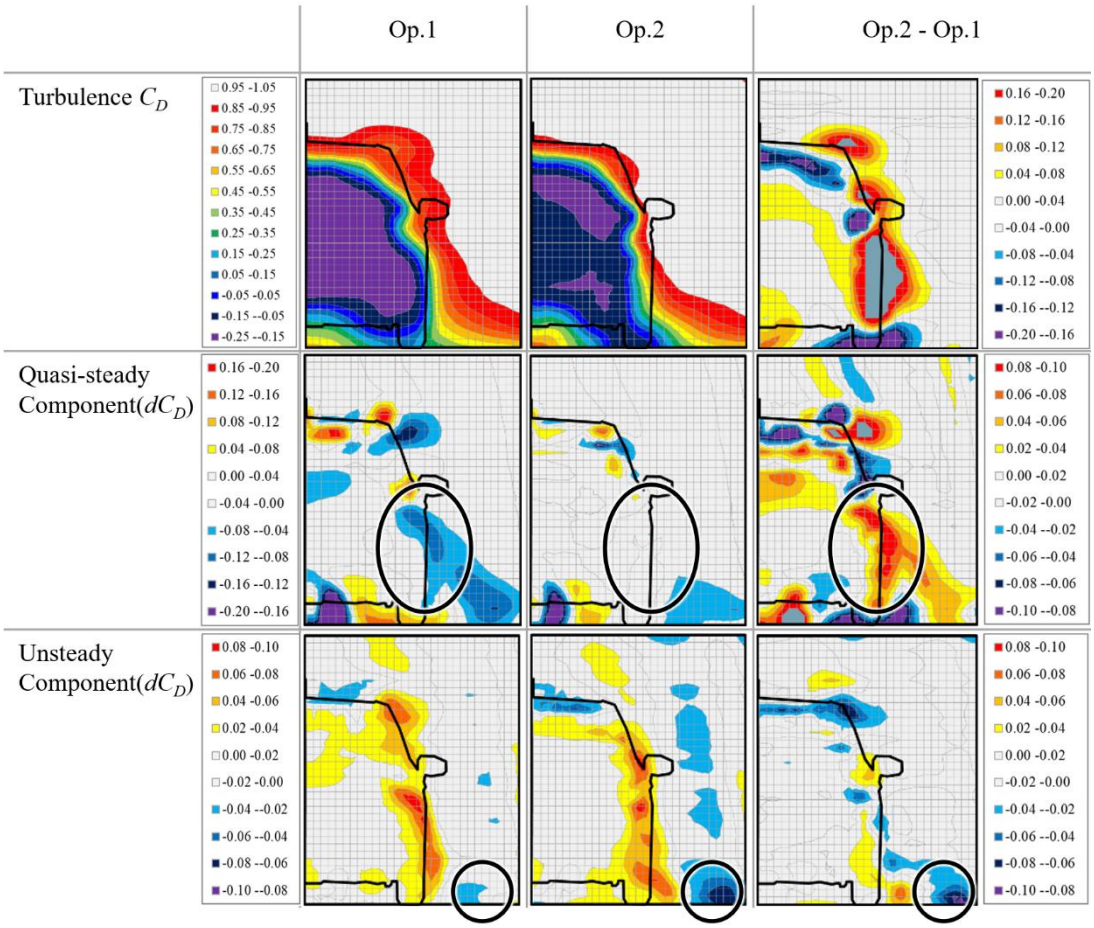

Figure 17 : the Quasi-steady component and the Unsteady component of total pressure in WAKE behind each option.

Figure 17 show the Quasi-steady component and the Unsteady component of total pressure in WAKE behind each option. At first, it is compared that the total pressures for the two options in turbulent. The result of Op.2, which is lower turbulence C_D than Op.1, the total pressure beside the vehicle is higher than that of Op.1. Next, it is compared that the Quasi-steady component of total pressures for the two options. Op.2 has not only lower C_D in turbulence, but also lower Quasi-steady C_D component than that of Op.1. The difference appears the Quasi-steady component of C_D total pressures beside the vehicle. This means that there is less separation of the Rear tire WAKE or side of Rear Bumper. On the other hand, Unsteady component of C_D at Op.1 works to reduce C_D 12ct and that at C_D at Op.2 works to reduce C_D 3ct. Therefore, the Unsteady component of total pressure of Op.2 is relatively lower than that of Op.1. According to this way of thinking, the Unsteady component of total pressure of Op.2 shows the lower total pressure. In specially, the difference beside the tire comes from Fr tire wake and it is predicted that the Fr tire separation point is different from both of options. The difference between both options is the Front strake, which acts to redirect the flow to the Front tire, thus affecting the separation location of the Front tire, thus matching the flow description.

These results suggest that reducing the Quasi-steady component also reduces the Unsteady component. In other words, in aerodynamic performance development that takes natural wind into account, improving the Yaw sensitivity of the C_D measured by the turn table sweep can also reduce the Unsteady component.

5 Conclusions

The static pressure gradient correction under TGS operating may not be appropriate, and it might not be necessary to apply it for C_D.

In order to reduce the effects of static pressure gradients that occur on the test vehicle due to various causes, it is best to make the length of the test section of the wind tunnel as long as possible, in line with the trend in state-of-the-art wind tunnels.

Improving the yaw sensitivity, Quasi-steady component, reduces Unsteady component.

6 Future work and limitations

This study suggested that reducing the Quasi-steady component also reduces the Unsteady component and improving the Yaw sensitivity of the C_D measured by the turn table sweep can also reduce the Unsteady component. However, there is a discrepancy between the scale wind tunnel results and the full scale wind tunnel results. The sign of the Unsteady component is opposite between the results in the scale wind tunnel and that in the full scale wind tunnel. The Unsteady component is negative in the scale wind tunnel, that is, it works in the direction of reducing C_D, whereas in the full scale wind tunnel it is positive, that is, it works in the direction of increasing C_D. The reason for this will be considered in the next study. On the other hand, the results of this study are focused on C_D effect from turbulence, and it is possible that TGS may be effective in terms of wind noise and stability.

7 Nomenclature and Abbreviations

WLTC	Worldwide-harmonized Light vehicles Test Cycle
EPA	The Environmental Protection Agency
C_D	the Drag Coefficient
TGS	Turbulence Generating System
TI	Turbulence Intensity
TL	Vortex scale length

FKFS ***swing***	FKFS side wind generator
CFD	Computational Fluid Dynamics
FSWT	Full Scale Wind Tunnel
SWT	Scale Wind Tunnel

8 Reference List

1. Where the Energy Goes: Gasoline Vehicles, https://www.fueleconomy.gov/feg/atv.shtml, 2023.
2. SAE International Light Duty Vehicle Performance &Economy Measure, “Road Load Measurement Using Onboard Anemometry and Coastdown Techniques,” SAE Standard J2263, Rev. Dec. 2008.
3. EPA Compliance Division. “Joint Technical Support Document: Final Rulemaking for 2017-2025 Light-Duty Vehicle Greenhouse Gas Emission Standards and Corporate Average Fuel Economy Standards,” EPA-420-R-12-901, August 2012.
4. UN Regulation No. 154 - Worldwide harmonized Light vehicles Test Procedure (WLTP)
5. Wordley, S. and Saunders, J., On-road Turbulence, SAE Technical Paper 2008-01-0475 (2008)
6. Wordley, S. and Saunders, J., On-road Turbulence: Part 2, SAE Technical Paper 2009-01-0002 (2009)
7. Schröck, D., Widdecke, N., and Wiedemann, J., “On-Road Wind Conditions Experienced by a Moving Vehicle,” in:Wiedemann, J. (ed.), Progress in Vehicle Aerodynamics and Thermal Management, Expert Verlag, Renningen, 2007.
8. McAuliffe, B. R., Belluz, L., & Belzile, M. (2014). Measurement of the On-Road Turbulence Environment Experienced by Heavy-duty Vehicles. SAE International Journal of Commercial Vehicles, 7(2), 685-702. doi:10.4271/2014-01-2451
9. Stoll, D., Schoenleber, C., Wittmeier, F., Kuthada, T. et al., "Investigation of Aerodynamic Drag in Turbulent Flow Conditions," SAE Int. J. Passeng. Cars - Mech. Syst. 9(2):2016, doi:10.4271/2016-01-1605.

10. Jessing, C., Wittmeier, F., Wiedemann, J., et al., “Characterization of the Transient Airflow Around a Vehicle on Public Highways” in:Wiedemann, J. (ed.), Progress in Vehicle Aerodynamics and Thermal Management, Expert Verlag, Renningen, 2019.

11. Cogotti, A., “Generation of a Controlled Level of Turbulence in the Pininfarina Wind Tunnel for the Measurement of Unsteady Aerodynamics and Aeroacoustics,” SAE Technical Paper 2003- 01-0430, 2003, doi:10.4271/2003-01-0430

12. Stoll, D., and Wiedemann, J., “Active Crosswind Generation and Its Effect on the Unsteady Aerodynamic Vehicle Properties Determined in an Open Jet Wind Tunnel”, SAE Technical Paper 2018-01-0722, 2018, doi:10.4271/2018-01-0722.

13. Onishi, Y., Ogawa, K., Sawada, J., Suwa, Y. et al., “On Road Fuel Economy Impact by the Aerodynamic Specifications under the Natural Wind,” SAE Technical Paper 2020-01-0678, 2020, doi:10.4271/2020-01-0678.

14. Fei, X., Kuthada, T., Wagner, A., and Wiedemann, J., “The Effect of Unsteady Incident Flow on Drag Measurements for Different Vehicle Geometries in an Open Jet Wind Tunnel,” SAE Int. J. Adv. Curr. Pract. Mobil. 4, no. 6 (2022):1999-2011, doi:10.4271/2022-01-0894.

15. Blumrich, R., Widdecke, N., Wiedemann, J., Michelbach, A. et al., "New FKFS Technology at the Full-Scale Aeroacoustic Wind Tunnel of University of Stuttgart," SAE Int. J. Passeng. Cars - Mech. Syst. 8(1):2015, doi:10.4271/2015-01-1557.

9 Acknowledgements

The authors would like to acknoledge the support from and collaboration with Dr.-Ing.Felix Wittmeier and Dr. Fei, X. at FKFS. The aouthors would like to thank FKFS for giving their permission to publish this papers.